Fibers and Polymers (2025) 26:739–754
https://doi.org/10.1007/s12221-024-00836-6

Online ISSN 1875-0052
Print ISSN 1229-9197

REGULAR ARTICLE

Sustainable Coloration and Functionalization of Silk Fabric Through Chinese Fringe Leaves (*Loropetalum chinense*) Extraction Using the Taguchi Method: An Alternative for Waste Management

Md Shazzat Hossain[1] · Syed Rashedul Islam[2,3] · Yahui Zhou[1] · Aimal Khan[1] · Haroon A. M. Saeed[1]

Received: 30 May 2024 / Revised: 22 November 2024 / Accepted: 21 December 2024 / Published online: 26 January 2025

Abstract

The escalating concern over the environmental impact of synthetic dyes in the textile industry has fueled a burgeoning interest in natural alternatives. This study aims to investigate the dyeing performance of silk fabric using dye extracted from Chinese fringe leaves (*Loropetalum chinense*), which are devoid of harmful chemicals, and to promote eco-friendly practices. The extraction process involved normal heating with crushed leaves, ensuring a purely natural dyeing method. Through experimentation, it was observed that higher dyeing temperatures, increased dye ratios, and longer dyeing durations enhanced color strength in the silk fabric treated with the Chinese fringe leaves dye. An orthogonal (L^{16}) Taguchi method was applied to determine the optimal dyeing conditions, emphasizing the significance of dye dosage and temperature in achieving maximum color strength. The initial parameter of *K/S* was 11.3 and the predicted parameter of *K/S* was 11.43, where the confirmation test value of *K/S* was 11.49 for the dyed fabric sample. Moreover, assessments of color fastness demonstrated satisfactory results ranging from good to excellent for washing, perspiration, rubbing, and light fastness. Fourier transform infrared analysis elucidated the interaction between dye molecules and silk fabric while scanning electron microscopy revealed the dye absorption by the silk fabric's surface. Thermogravimetric analysis revealed differences in thermal properties between dyed and undyed silk fabric, with dyed fabric exhibiting lower melting points and reduced thermal stability. Additionally, the dyed silk fabric exhibited decreased air permeability of 122 ± 2 mm/s with an increased protection factor of 317.9 against UV and sun rays compared to its undyed silk fabric sample. In inference, the dye extracted from Chinese fringe leaves possessed a favorable affinity for silk fabric, presenting a promising alternative to synthetic dyes for sustainable coloration and functionalization in the textile industry.

Keywords Silk fabric · Natural dye · Taguchi method · Sustainability · Textile dyeing process

1 Introduction

Nowadays, global attention is firmly fixed on achieving sustainable development goals with a significant focus on reducing pollution levels across various industries [1, 2]. One sector under intense scrutiny is textile dyeing, where the use of toxic chemicals causes substantial environmental damage [3]. Though synthetic dyes are favored for their low cost, ability to produce vibrant colors, and excellent colorfastness compared to natural dyes, however, they pose grave threats to ecosystems [4, 5]. Their impact spans agricultural desertification, climate change, water systems, and global societal balance, exacerbated by the toxic substances involved in their production, some of which are carcinogenic [6, 7]. Consequently, many countries have implemented strict bans on synthetic dyes to safeguard the environment.

✉ Syed Rashedul Islam
syed.islam@uttarauniversity.edu.bd; sri060791@gmail.com

✉ Haroon A. M. Saeed
haroonsaeed75@gmail.com

1 Key Laboratory of Green Processing and Functional New Textile Materials of Ministry of Education, Wuhan Textile University, Wuhan 430200, People's Republic of China

2 Department of Textile Engineering, Uttara University, Dhaka 1230, Bangladesh

3 Department of Textile Engineering, National Institute of Textile Engineering and Research (NITER), University of Dhaka, Dhaka 1350, Bangladesh

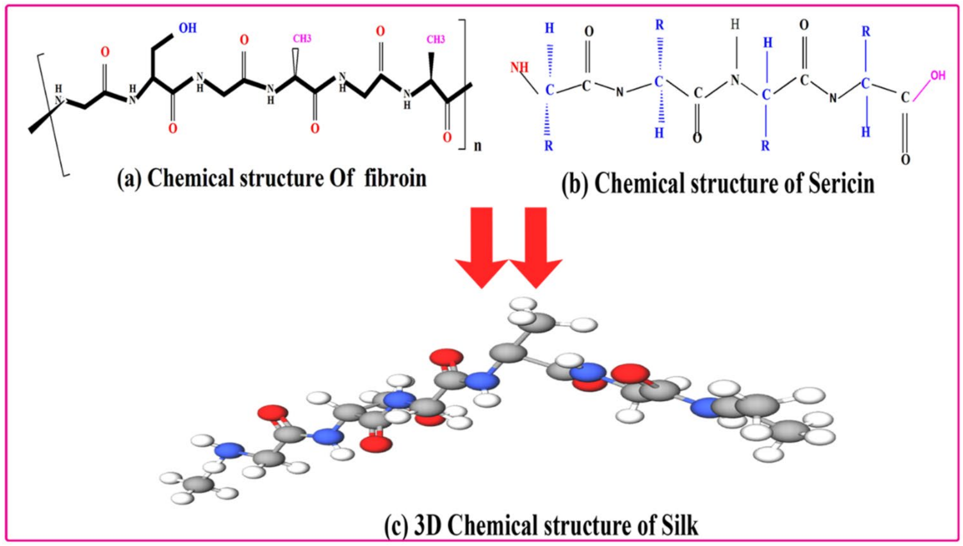

Scheme 1 **a** Molecular structure of fibroin, **b** molecular structure of sericin, **c** 3D chemical structure of silk

In this context, natural dyes emerge as a promising alternative, as underscored by recent research [8, 9]. Because they are readily available and easily obtained from natural sources such as tree bark, bark, fruits, and leaves [10]. Using natural dyes in the textile industry does not hamper waste disposal and provides soothing colors while benefiting people worldwide [11]. They are also considered natural boons as most of them are essential ingredients of pharmaceutical and Ayurvedic remedies [12]. Moreover, the shift towards natural dyes not only addresses environmental concerns but also aligns with global efforts towards sustainability, marking them as valuable assets in fostering a greener future for all.

Silk is called the "Queen of Fibers" due to its fine and silky texture, high mechanical performance, luster, lightweight, excellent draping, and moisture retention [13]. According to the observation, Chinese fringe leaves can be used to dye natural fabrics such as silk, wool, and cotton. While various mordants are typically employed to achieve a range of colors, however, it is also feasible to dye without using any mordant [14]. Silk fabrics generally become hydrophilic due to the low glass transition temperature, low melting point, soft molecular structure, and high polarity of silk fibers. The hydrophobicity of silk fabric causes easy dye penetration into silk fabric. The chemical structure of fibroin, sericin, and 3D molecular structure of silk have been shown in Scheme 1a, b, c, respectively.

Currently, textile researchers are trying to find new plant sources that can naturally produce dyes and pigments to solve environmental problems. Various previous studies have shown that fabric dyeing with natural dyes generally exhibits high cost, low color strength, and poor fastness properties [15, 16]. To solve this problem, a new plant called Chinese fringe leaves (*Loropetalum chinense*) has been studied in this research that can open the door to textile industry as a new source of natural dyes. Chinese fringe leaves (*Loropetalum chinense*) are a genus of four species of small trees in the witch-hazel family found in China, Japan, and Southeast Asia. The plant has a long history of use as a beautifier along roadsides, in universities, and various offices. As this plant has no other use, the growing leaves of this plant are cut every month and thrown away as excess waste. However, no researcher has tried dyeing fabric with this leaf extract before. Although Zhang et al. did a comprehensive analysis and revealed the mechanism of color formation of Chinese fringe leaves with phenotypic/anatomic observations [17]. Nevertheless, no satisfactory research was found from them.

Many researchers worked on the dyeing of silk fabrics with other natural dyes. Khan et al. found in a previous study that camphor (*Cinnamomum camphora*) leaf extract was effectively used to dye silk fabric using the exhaust dyeing method [18]. Additionally, their other research demonstrated that functional wool fabric was successfully dyed with *Cinnamomum camphora* leaf extracts when converted into powder form [19]. Uddin et al. investigated in their previous study that different types of mordants mixed with mango leaf extract and onion skin exhibited very good color fastness when applied to silk fabrics [20, 21]. Do et al. explained in a previous study that dye extracted from *Laccifer lacca* Kerr. altered the functional properties of silk fabric when applied. [22]. Punrattanasinan et al. employed mangrove bark extract as a source of natural dyes to color the silk fabric [23]. This extracted dye was applied by an exhaustion dyeing process where aluminum potassium sulfate, ferrous sulfate, copper sulfate, and stannous chloride were used as mordants. Teklemedhin et al. investigated the process of sustainable dyeing of silk fabric with natural dye extracted with an aqueous extraction method from the *Cassia singueana* plant [24]. Dayioglu et al. investigated the oxygen plasma pre-treatment at a low frequency on silk fabric dyed with

Sambucus ebulus L. Plant extract [25]. Sasivatchutikool et al. studied the effects of dyeing silk fabric with natural dye extracted from *Cassia Fistula* ripe pods with pre-mordanting and post-mordanting processes [26]. However, no research work has been conducted on dyeing organic non-woven silk fabrics using Chinese fringe leaves to date.

Therefore, in this study, a silk fabric was dyed using sustainable and eco-friendly natural dyes extracted from Chinese fringe leaves. From this extensive research, it was found very well to excellent washing fastness, light fastness, rubbing fastness, and perspiration fastness of dyed silk fabric. The scanning electron microscopy (SEM) images and optical microscopic images indicated the presence of dye particles on the silk fabric surfaces without any damage. The dyed silk fabric sample was also evaluated with air permeability and sun ray protection. Therefore, using Chinese fringe leaf extract to dye silk fabrics could be the best alternative to synthetic dyes in the textile sector in terms of environmental matters.

2 Experimental

2.1 Materials

A 100% woven silk fabric weighing 100 g/m^2 was supplied from a reputed fabric manufacturing industry in Shanghai, China. Chinese fringe flower leaves were collected from a garden at Wuhan Textile University, China. The Titanyl Sulfate ($TiOSO_4$; CAS Number: 7787-24-9) was purchased from Shanghai, China.

2.2 Dye Extraction and Dyeing Process

2.2.1 Extraction of Natural Dyes

The collected Chinese fringe flower leaves were first washed with normal water to remove dust for dye extraction. Then, these leaves were placed in direct sunlight for 24 h to dry. After drying, the leaves were completely made into powder using a grinding machine. Then, these powders were taken in a beaker and mixed with water in a ratio of 1:10. The entire dye extraction process was carried out in aqueous medium [27, 28]. The dye extraction process was carried out in a dyeing bath at 90 °C for 30 min. The extracted dyes were filtered twice through a fine filter to obtain a clear and liquid dye solution. Then, the obtained dyes were stored for further dyeing process. The dye extraction process through a schematic diagram is illustrated in Scheme 2.

2.2.2 Dyeing Process

The dyeing process was carried out with different parameters and conditions, where an orthogonal (L^{16}) Taguchi technique was applied to determine the best condition for silk dyeing. The dyeing process was carried out through three factors: temperature, time, and dye dosage followed by Table 1. However, the pH value was 4 for each experiment. A normal close bath system and a standard quality lab-based oven were used from Nanbei Instrument Limited, China. After the dyeing process, the fabric samples were normally rinsed with deionized cold water and then dried in a dryer.

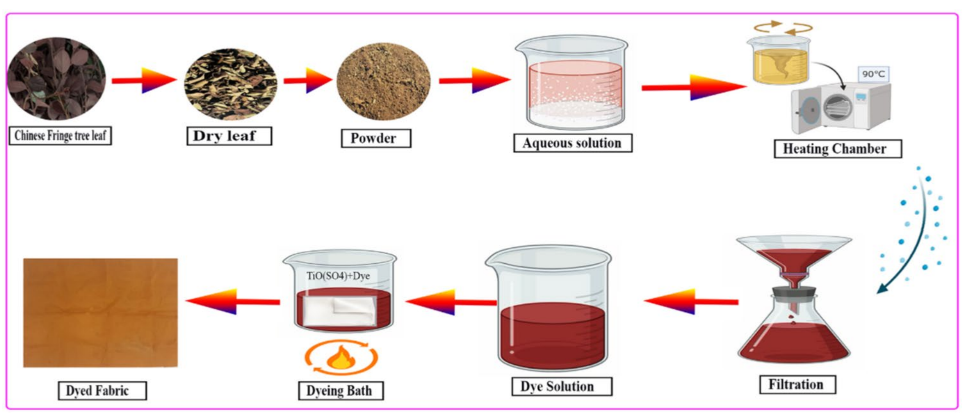

Scheme 2 A schematic presentation of dye extraction and dyeing process

Table 1 Parameters and their levels of the L^{16} orthogonal experiment scheme

Symbol	Parameters	Unit	Level 1	Level 2	Level 3	Level 4
A	Temperature	°C	80	90	100	110
B	Dyeing time	min	80	90	100	110
C	Dye dosage	%, o.w.f	8	12	16	20

A = Temperature; B = Dyeing time; C = Dye dosage

2.3 Basic Concept of the Taguchi Method

Taguchi method was considered a statistical method that selected the best research method and evaluated the significance between different factors [29, 30]. The orthogonal Taguchi method assessed the various factors in such a way as to reduce the cost and time of testing. The main purpose of this test was to select the best conditions for the study. An orthogonal Taguchi technique was applied to determine the optimum dyeing condition based on color strength. Here, the signal-to-noise (*S/N*) ratio was considered the fundamental basis of the Taguchi technique, which was used to determine the characteristic quality of the final product. The larger S/N ratio approach was used under the Taguchi method. Equation (1) was used to calculate the larger S/N ratio [31].

$$S/N = -10\log\left(\frac{1}{n}\sum_{i=1}\frac{1}{y_i^2}\right) \quad (1)$$

where $y_i = i$th experiment in the design, and n = whole number of tests. The *S/N* ratio is expressed in decibels or delta (dB).

2.4 Measurement and Characterization

The dyed silk fabric and dye solution were examined using color strength (*K/S*), scanning electron microscopy (SEM), Fourier transform infrared spectroscopy (FTIR), optical microscopy, EDS, TGA, DTG, UV–Visible spectrophotometer, color fastness (to light, wash, wet and dry-rub, and perspiration), air permeability, and UV and sun protection properties.

2.4.1 Fourier Transform Infrared (FTIR) Spectroscopy Measurement

The functional group of silk fabric was measured using a Bruker Alpha and Tensor 27 FTIR spectrophotometer (Shimadzu, Japan). FTIR depends on the amount of transmission and absorption of infrared radiation passed through a sample. The signal detector produced some peaks of functional group called as "fingerprint". The range of the wavelengths was 4000–500 cm^{-1}.

2.4.2 Color Strength Measurement of Silk Fabric

The reflectance spectrophotometer (Data color 650, China) was used to measure the color strength of the dyed silk fabric sample. Kubelka–Munk theory was used to determine the depth of the color considering the following Eq. (2) [32].

$$K/S = \frac{(1-R)^2}{2R} \quad (2)$$

where K = absorption co-efficient; S = scattering co-efficient of dyes; R = reflectance percentage. Colorimetric properties of the dyed silk fabrics (L^*, a^*, b^*, c^*, and $h°$) were evaluated according to the AATCC test method with illuminant D65 and 10° observers [33].

2.4.3 Color Fastness Measurement of Silk Fabric

The washing fastness was measured with a gyro washing fastness tester (James Heal, UK). 2 g/L soda ash and 5 g/L detergent were used to measure the color fastness to wash (ISO 105 C03:2013). The colorfastness to perspiration, rubbing, and light were measured using the standards ISO 105-E04:1994, ISO 105-X12:2016, and ISO 105-BO2:2013, respectively.

2.4.4 Scanning Electron Microscopic (SEM) Measurement

Scanning electron microscopy (SEM) was measured with the SEM tester (JEOL 6460LV, Tokyo, Japan). The SEM images were captured with 5.0 kV of accelerating voltage using the JSM-6610LV. This machine works with some signals of light-emission energy electrons. Surface morphology, chemical composition, and crystalline structure were evaluated by the obtained signal of SEM images.

2.4.5 Optical Microscopy

The optical microscopic view was measured with LEICA Dm-2500 LED Microscope, Wetzlar, Germany with high-performance fluorescence. The normal microscope was able to take images 40× to 1000×.

2.4.6 Thermogravimetric Analysis (TGA)

The thermal stability for both dyed and undyed silk fabric was carried out using a TG analyzer (Model-STA300, Hitachi High-Tech Science Corporation 1-17-1 Toranomon, Minato-ku, Tokyo, JAPAN). The analysis was carried out up to 600 °C (10 °C/min) with a nitrogen environment (40 mL/min). For TGA analysis, 2–5 mg was used for both samples, determining the weight loss with temperature. TGA curves and DTG curves indicated the relation between weight loss and temperature.

2.4.7 Ultraviolet–Visible (UV–Vis) Spectroscopy Measurement

The ultraviolet spectrum was evaluated by ultraviolet–visible (UV–Vis) spectroscopy (UV-3600 plus, UV–VIS–NIR spectrophotometer, Shimadzu, UK). The UV spectrum peak was studied according to different material ratios and p^H.

2.4.8 Air Permeability Analysis

Air permeability for both dyed and undyed silk fabrics was determined using the GLOMRO fabric Air Permeability Tester (Model: YG461E, GLOMRO, Shanghai, China) with ASTM D737 methods. The test results were presented as mm/s. A 20 cm^2 test area was utilized for the testing, and the samples' air permeability was assessed at 100 Pa of air pressure.

2.4.9 UV Protection Properties

The UV blocking testing was carried out according to the AATCC 183 test method using a UV transmittance analyzer (Ultraviolet Prevention Performance Tester YG(B)912E, China). The spectra of wavelength were recorded in the range of 290–400 nm.

3 Result and Discussion

3.1 Taguchi Model Analysis Based on Color Strength

The experimental data for the Taguchi analysis was obtained by an orthogonal experimental scheme using an L^{16} (4^3) array, where the dye dosage was 8–20 (o.w.f) [34]. The values and ranges of the parameters utilized in the orthogonal experimental design are presented in Table 1 by following the L^{16} (4^3) array of the orthogonal experimental scheme.

On the other hand, the obtained *K/S* values of the sample and S/N ratio values are presented in Table 2. The maximum color strength of 11.3 and S/N ratios of 21.0616 were found with temperature at 80 °C, time at 110 min and dye dosage at 20% (o.w.f). The possible reason to get maximum color strength was maximum color absorption in this condition. On the other hand, the lowest color strength was found to be 9.6, whose parameters were presented in test number 16.

Table 2 L^{16} orthogonal array of factors, experimental data, and S/N ratios

Exp. no	A	B	C	*K/S*	*S/N* ratio (dB)
1	80	80	8	9.9	19.9127
2	80	90	12	10.3	20.2567
3	80	100	16	10.6	20.5061
4	80	110	20	11.3	21.0616
5	90	80	12	10.7	20.5877
6	90	90	8	10.5	20.4238
7	90	100	20	11.2	20.9844
8	90	110	16	10.8	20.6685
9	100	80	16	10.4	20.3407
10	100	90	20	10.9	20.7485
11	100	100	8	9.8	19.8245
12	100	110	12	10.1	20.0864
13	110	80	20	10.5	20.4238
14	110	90	16	10.2	20.1720
15	110	100	12	9.8	19.8245
16	110	110	8	9.6	19.6454

A = Temperature; B = Dyeing time; C = Dye dosage

3.1.1 Assessment Table for S/N Ratios

For optimal condition evaluation through the orthogonal Taguchi technique, S/N ratios obtained from color strength were considered as the fundamental basis [35]. The response for S/N ratios (color strength) is presented in Table 3.

Here, the best conditions were evaluated by representing the average maximum S/N values of each factor through the delta statistic. It was seen from Table 3 that, the dye dosage and temperature had a significant effect on the dyeing process, whereas the effect of time was less observed. In the dyeing process, dye dosage was ranked 1st with the highest delta value of 0.85, temperature was ranked 2nd with 0.65, and time was ranked 3rd with 0.12.

Table 3 Response for S/N ratios (color strength)

Level	A	B	C
1	20.43	20.32	19.95
2	20.67	20.40	20.19
3	20.25	20.28	20.42
4	20.02	20.37	20.80
Delta	0.65	0.12	0.85
Rank	2	3	1

A = Temperature; B = Dyeing time; C = Dye dosage

3.1.2 Assessment of Main Effect Plot

The main effect plot was crucial for determining the best factor and optimal condition using a line graph [36]. From the main effect plot (see, Fig. 1), it was evident that temperature and dye dosage had a very high effect on the dyeing process, whereas dyeing time had very little effect. The figure also indicated that the best conditions were A2B2C4 (where A2 = 90 °C, B2 = 90 min, C2 = 20% dye dosage), specified as the optimal dyeing condition based on color strength. Mostly, color strength depended largely on dyebath temperature and dye dosage. It was observed that maximum color strength was achieved when the temperature was raised from 80 to 90 °C. Further increased to 100 and 110 °C did not improve color strength. At 90 °C, the fiber structure

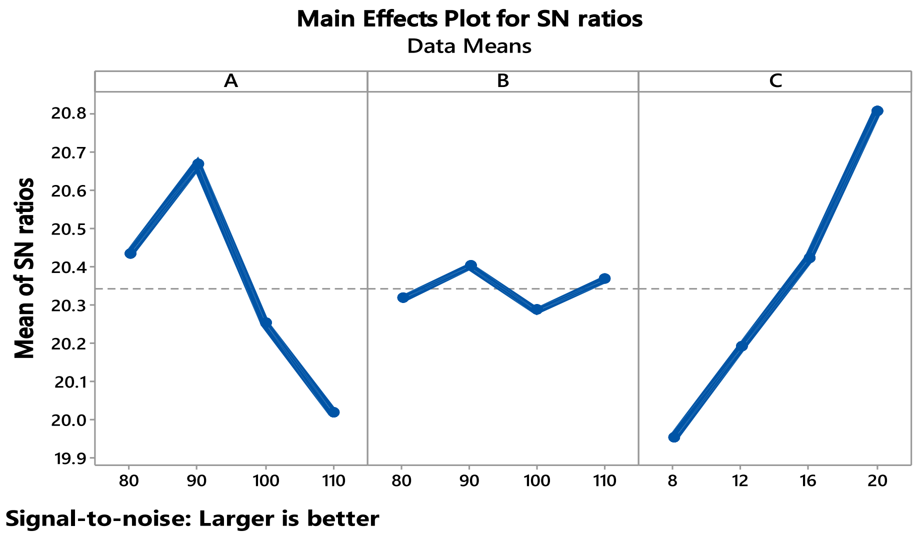

Fig. 1 Main effect plot for S/N ratio of color strength

opened to the maximum extent, allowing it to absorb the greatest amount of color.

When the temperatures were 100 and 110 °C, the fiber became more swollen, and the absorbed dyes began to desorb. As a result, the optimum color strength was achieved at 90 °C. Dyeing time was not a significant factor in the dyeing process, but the best color strength was obtained at 90 min. It decreased slightly to 100 min and then increased again at 110 min. For the Chinese fringe leaf extract dye dosage, color strength increased continuously with the amount of dye dosage. The dye dosage was progressively increased to 8%, 12%, 16%, and 20% (o.w.f), with the best color strength achieved at 20% dye dosage.

3.1.3 Assessment of Interaction Plot

The interaction effects plots for S/N ratios provided a qualitative understanding of the degree of interaction between two parameters [37]. Here, the parallel lines indicated weak interaction in the dyeing process, while non-parallel lines indicated moderate interaction. In Fig. 2, factor (A) showed that the three lines were asymmetric, indicating a strong

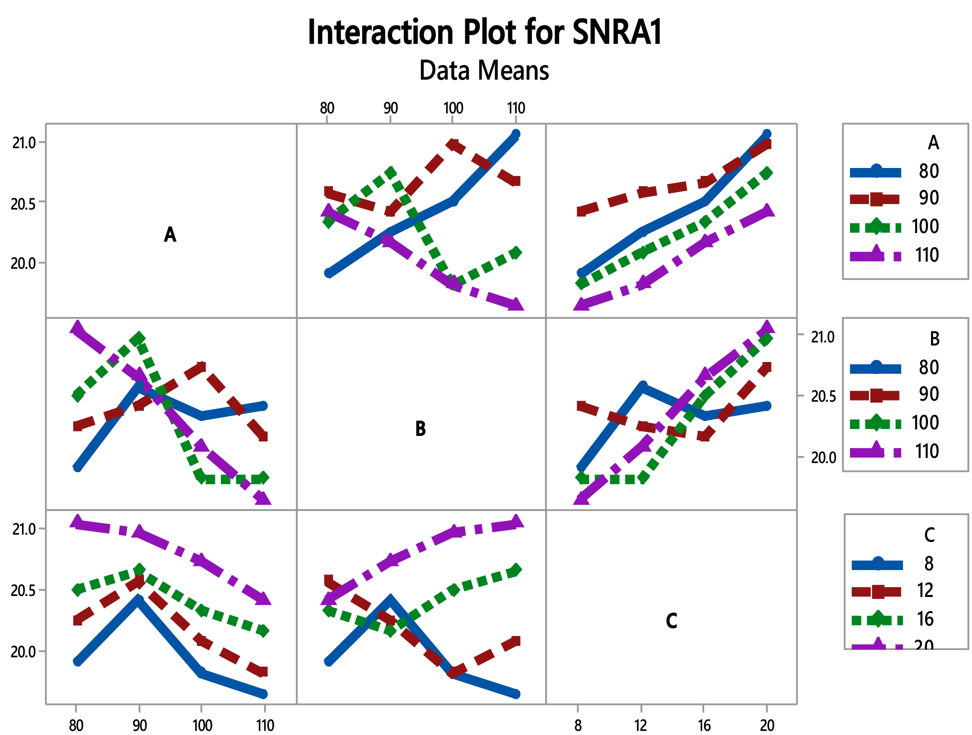

Fig. 2 Interaction effect plot for S/N ratio of color strength

interaction in the dyeing process. Factor (B) revealed a very weak interaction. Additionally, Fig. 2 (factor (C)) displays non-parallel lines, suggesting that this factor had a significant effect on the coloration.

3.1.4 ANOVA

A statistical method (ANOVA) was capable of finding the impact of process factors after analyzing experimental data. This method worked well for determining the percentage of each factor in the dyeing process. ANOVA was used to calculate the *F*-values, which were the ratio of the mean square error to the regression mean square. The *F*-values represented the ratio of variance due to an error term to variance due to the influence of a factor. The *p*-value was the most important metric, determining whether a factor was significant or not. If the *p*-value was less than 0.05, it was considered significant. Table 4 shows the ANOVA for the S/N ratio based on color strength. Dye dosage demonstrated a higher impact on color strength due to a high *F* value (37.95), and temperature also had a greater influence on the dyeing process with the second-largest *F* value (13.57). Therefore, dye dosage and temperature were significant in the dyeing process. In contrast, dyeing time was not significant due to its lower *F* value.

3.1.5 Assessment of Residual Plots

The residual plots for S/N ratio of color strength from the dyed silk fabric are displayed in Fig. 3. The normal probability plot exhibited that the values generally fell on a straight line, with most points lying very close to this line, indicating that residual errors were distributed normally during the dyeing process. Additionally, the residuals plot versus fit graph showed that all lower points were very close to the zero line, while the upper points appeared to fall randomly near the zero line, confirming the significance of the residuals. The large number of inspections was confirmed by the histogram bar chart. Furthermore, the residuals versus observation order plot demonstrated that the observed residuals were distributed randomly around the zero line, indicating that the residuals were dependent on the dyeing process [38].

Table 4 ANOVA for the S/N ratio (color strength)

Source	DF	SS	MS	*F*-Value	*P*-Value	Remarks
A	1	0.55750	0.55750	13.57	0.003	Significant
B	1	0.00021	0.00021	0.01	0.944	Not Significant
C	1	1.55886	1.55886	37.95	0.000	Significant
Residual error	12	0.49292	0.04108	–	–	–
Total	15	2.60949	–	–	–	–

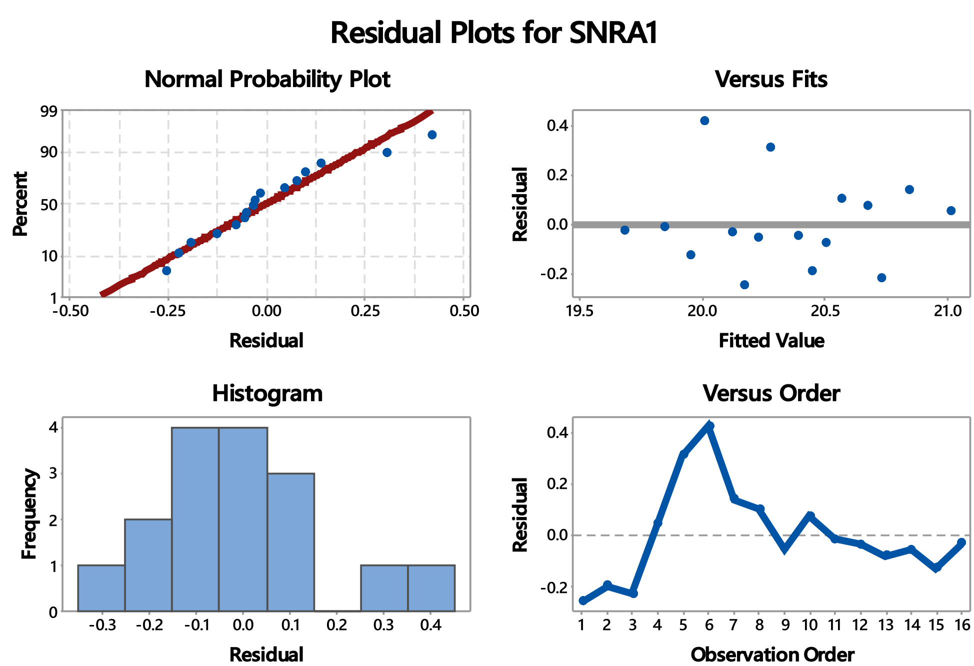

Fig. 3 Residual plots for the S/N ratios of color strength

3.1.6 Fitted Plot Assessments

The experimental and predicted S/N ratio percentages were determined by using a plot line graph, as presented in Fig. 4.

The residual position near the diagonal line evaluated the significance of the model. The residuals located in this graph were very close to the diagonal line, indicating the significance of the model in the dyeing process [39]. The graph also showed a strong agreement of $R^2 = 81.1$ and an adjusted $R^2 = 79.8\%$, respectively, between the experimental and predicted values. Furthermore, a strong relationship was found in the dyeing process indicated by the Pearson correlation coefficient, which was 0.811 with a p-value of 0.000.

3.1.7 Confirmation Test

A confirmation test was performed to verify the validity of the final results of the Taguchi technique. The main purpose of this analysis was to confirm all data, tests, and responses. The results of the confirmatory tests are presented in Table 5. According to the confirmation experiment, the initial parameter of *K/S* was 11.3, the predicted value of *K/S* was 11.425, and the confirmed value of *K/S* was 11.49. The confirmation by the matrix experiment was actually achieved under ideal conditions. After determining the optimal conditions, the optimization process was verified. The results obtained (Improvement in S/N ratio = 0.1448) showed that there was a significant improvement in color intensity which indicated the success of the systematic statistical experimental design. Therefore, overall, after successfully evaluating the Taguchi analysis the best optimization sample was treated with 90 °C temperature, 90 min time, and 20% dye dosage to get a maximum color strength (*K/S*) value of 11.49.

Table 5 Results of the confirmation experiment

Level	Initial parameters A1B4C4	Prediction A2B2C4	Confirmation experiment A2B2C4
K/S	11.3	11.425	11.49
S/N	21.0616	21.1875	21.2064
Improvement in S/N ratio	–	0.1448	–

3.2 Characterization of Dye and Treated Fabric

3.2.1 Fourier Transform Infrared (FTIR) Analysis of Dye

Chinese fringe leaves extracted dyes were evaluated with FT-IR analysis, as presented in Fig. 5. The dyed samples were assessed in two ways where Fig. 5a was for only Chinese fringe leaves extracted dye and Fig. 5b was for the solution of Chinese fringe leaves dye with titanyl sulfate ($TiOSO_4$). However, both of the dye samples displayed approximately similar peak for similar stretching vibration. Chinese fringe leaves extracted dye exhibited the FT-IR spectrum peaks at 3214 cm^{-1} for hydroxyl groups bond (–OH) [40]. Other asymmetrical stretching vibration peaks indicated the carbon–hydrogen bond (C–H) at 2951 cm^{-1}. The band at 1635 cm^{-1} was assigned for the stretching vibration of the Amide I bond (amide C=O stretch: proteins, β-sheet). These functional groups indicated the presence of proteins in the Chinese fringe leaves extraction. The wavenumber at 1050 cm^{-1} was specified C–O–C functional group for the symmetric stretching vibration [41]. Bending vibration at 875 cm^{-1} directed the functional group of carbonates (–C=O). According to the previous study, it was found that

Fig. 4 The fitted line for the experimental and predicted S/N ratios

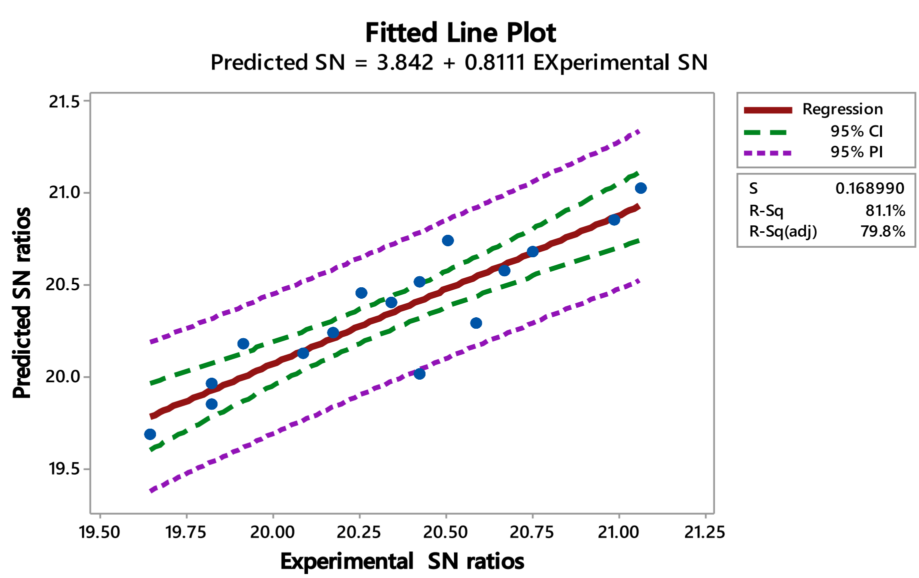

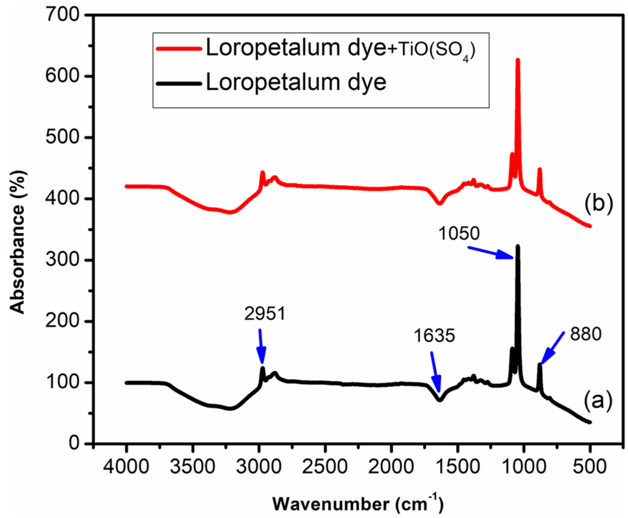

Fig. 5 FTIR analysis of **a** Chinese fringe leave extract and **b** Lorpetalum dye and Titanyl Sulfate ($TiOSO_4$) solution

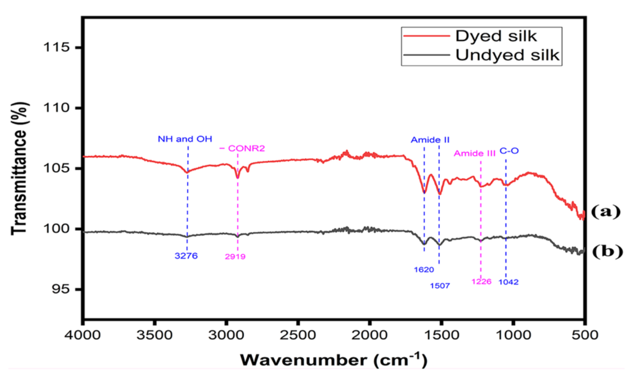

Fig. 6 Fourier Transform Infrared (FTIR) spectra of: **a** pure silk undyed fabric and **b** dyed silk fabric

different molecules were influenced by each other through vibronic coupling which indicated the absorption spectra with anthraquinones and other coloring groups [42].

3.2.2 Fourier Transform Infrared (FTIR) Analysis of Silk Fabric

The functional groups on the surface of dyed fabric and undyed silk fabric were examined using Fourier transform infrared spectroscopy (FT-IR) with attenuated total reflectance (ATR) mode [43]. FT-IR analysis of dyed and undyed fabric sample is shown in Fig. 6. Three important peaks were found in the dyed sample at 3276 cm^{-1}, 1620 cm^{-1}, and 1507 cm^{-1}. The wavenumber at 3276 cm^{-1} was for stretching vibrations of the N–H and O–H bonds in protein fiber. The wavenumber at 1620 cm^{-1} was for stretching of the amide group I (–$CONR_2$) and the wavenumber at 1507 cm^{-1} was for stretching of the amide group II. The represented peak at 1226 cm^{-1} represented the amide III. The weak peaks at 1284 cm^{-1} characterized the β-sheet structure of silk. The peaks at 2919 cm^{-1}, 1045 cm^{-1}, and 500–700 cm^{-1} were assigned due to the stretching vibration of C–H, C–O, and C–C, respectively. These FT-IR peaks of silk fabric were also observed by another previous study [44]. Both the dyed and undyed silk fabric samples showed almost the same FT-IR peaks with a very small significant change. However, the peak at 1042 cm^{-1} represented the C–O stretching vibration that indicated the strong bond between dyes in silk fabric. When the organic silk fabric was dyed with Chinese fringe leaves extracted dye, new peaks indicated a chemical reaction between the dye and the silk fabric which confirmed the possibility of bonding during the dyeing process.

3.2.3 Scanning Electron Microscopy (SEM) Analysis

The scanning electron microscope (SEM) was used to examine the surface morphology of samples of dyed and undyed silk fabric. After taking pictures at various magnifications, the potential change in the morphological structure of dyed and undyed silk fabric was examined and compared the structure for both dyed and undyed fabric. The scanning electron microscopic images provided additional proof that the surface of organic silk fabric effectively absorbed the dye (Chinese fringe leaves extract). Figure 7 represents the pictures captured by a scanning electron microscope of both dyed and undyed silk fabric samples. However, the fabric was dyed at a medium temperature of 90–120 °C and that was why the fabric surface structure was not damaged. There was a clear difference between the dyed and undyed silk fabric samples, as shown in the SEM images. In comparison to the dyed fabric samples in Fig. 7a–c, the undyed samples surface characteristics in Fig. 7d–f seemed to be considerably smoother and more polished. Because of the presence of the dye, the dyed silk fabric sample showed uneven morphology at the microscale. The interaction between the dye molecules and the organic silk fabric during the dyeing process was probably the main cause of this roughness [45]. The morphology examination also showed that the organic silk fabric sample did not show any signs of color buildup. The result exhibited that Chinese fringe leaf extract was successfully used to color organic silk fabric and the dye was evenly absorbed by the fabric.

According to SEM and EDS results, Fig. 8 reveals the EDS mapping for the undyed silk fabric where the mapping indicated "how the nitrogen components of the silk fabric equally distributed throughout the material". On the other hand, a small change was found in the distribution of the nitrogen compound for dyed silk fabric, as shown in Fig. 9. This change of compound clearly proved that

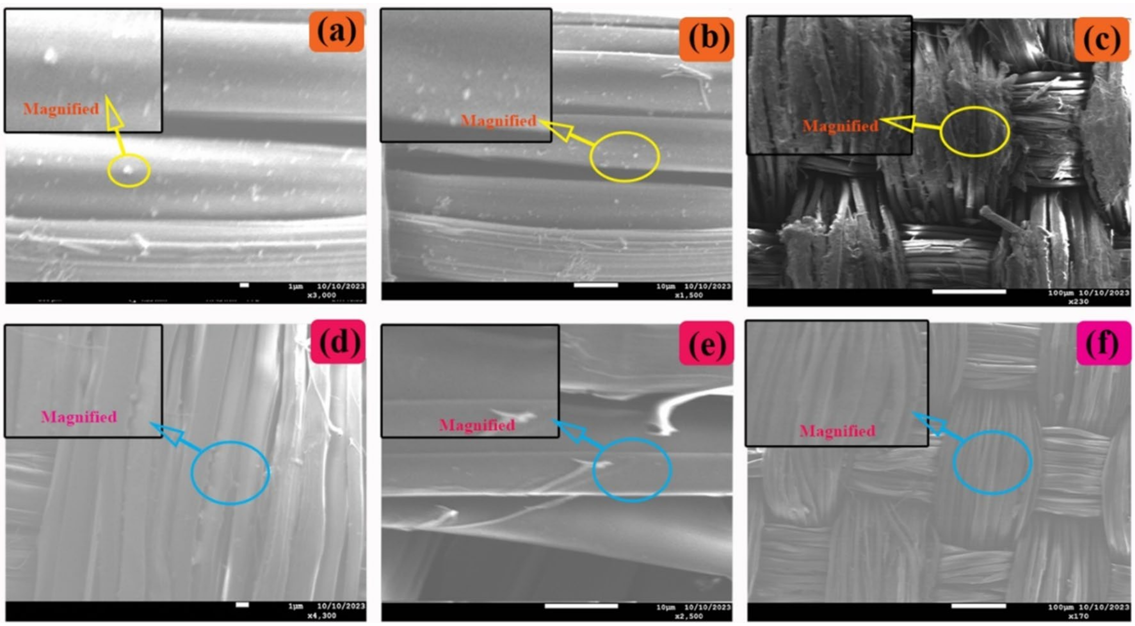

Fig. 7 SEM images of dyed (**a–c**) and undyed (**d–f**) silk fabric at different magnifications

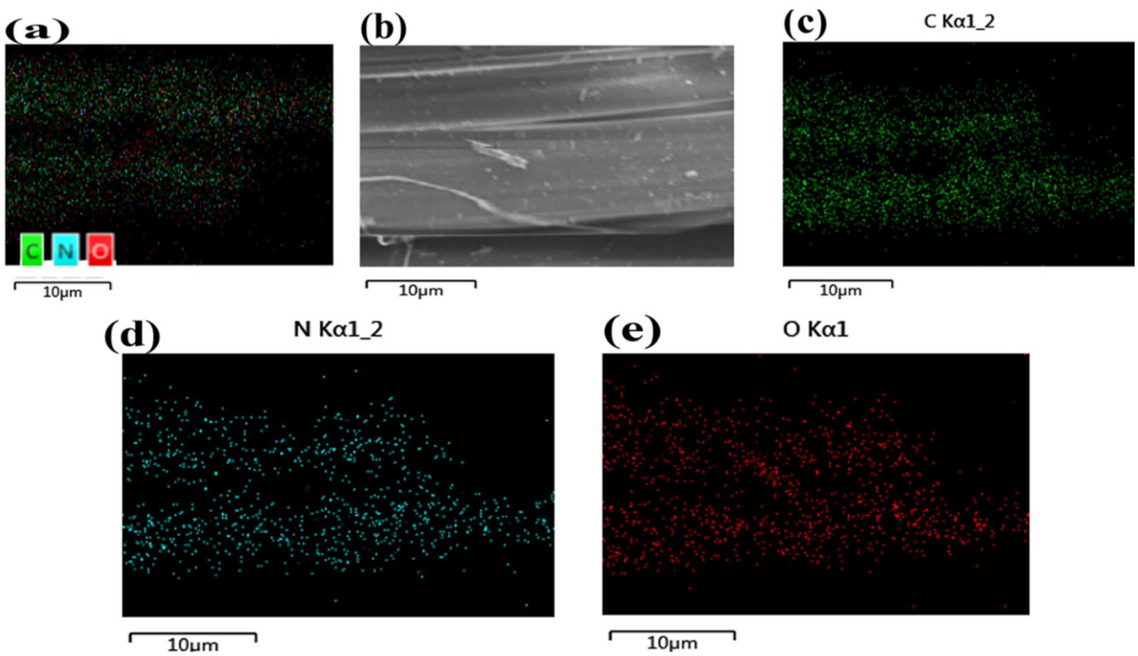

Fig. 8 EDS analysis of undyed silk fabrics: a = elemental micrograph; b = SEM photograph; c = distribution map of C (Carbon); d = distribution map of N (Nitrogen) element; e = distribution map of O (Oxygen) element

the dye was effectively penetrated into the fabric. In addition, silk fabric partially absorbed some new particle in the dyeing process (Ti and S). The EDS results were also confirmed by the previous study [46].

3.2.4 Optical Microscopic Analysis

The optical microscopic test was used to get a real microscopic image of a sample with 40× to 1000×. Figure 10 represents the microscopic images of dyed and undyed silk

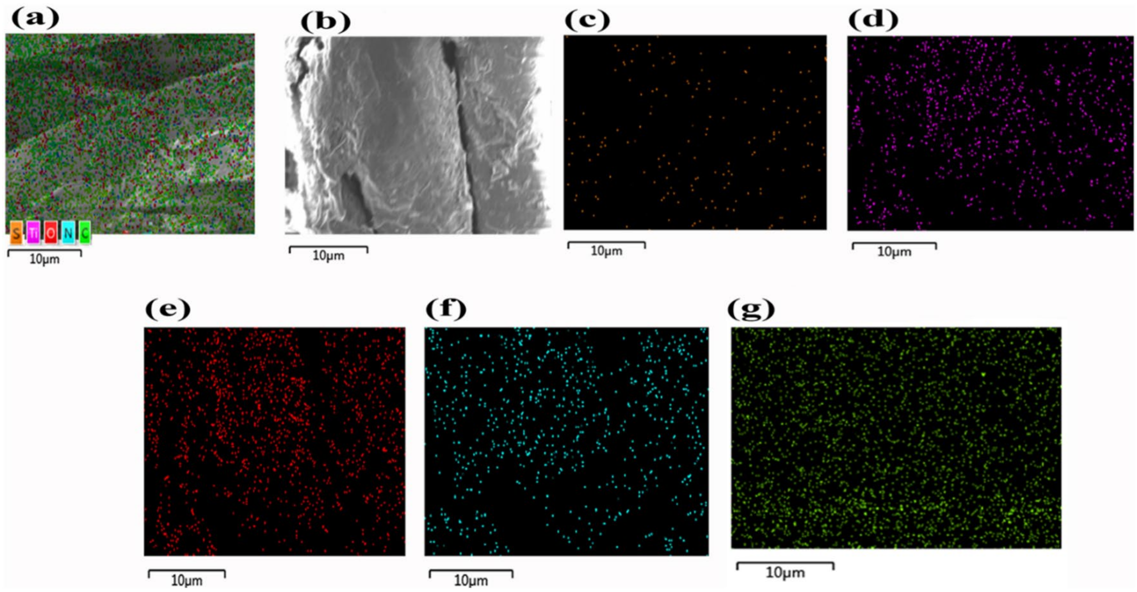

Fig. 9 EDS analysis of dyed silk fabrics **a** elemental micrograph; **b** SEM photograph; **c** distribution map of S (Sulfur) element; **d** distribution map of Ti (Titanium); **e** distribution map of O (Oxygen); **f** distribution map of N(Nitrogen); **g** distribution map of C (Carbon)

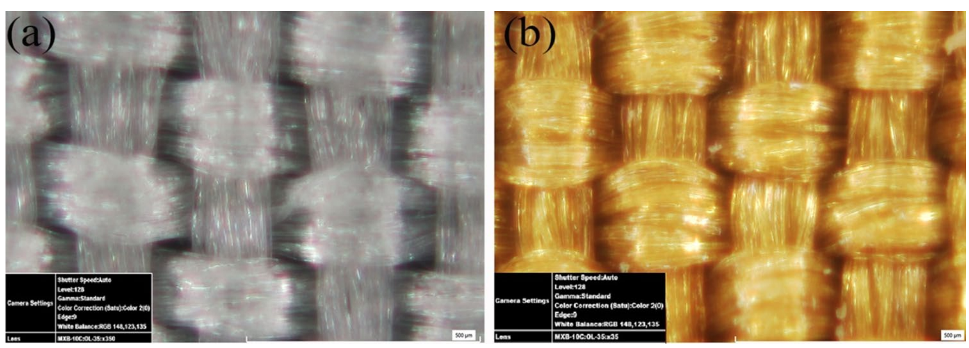

Fig. 10 Optical microscopic images of **a** undyed silk fabric and **b** dyed silk fabric

fabric. The images, Fig. 10a displays the undyed silk fabric sample structure (plain design with 1/1). Besides, similarly, the dyed silk fabric samples, Fig. 10b presents the same structure with different shades of color. This optical microscopic analysis suggested that the color intensity and the depth of the color in the dyed sample presented maximum color absorption with light shade. Overall, the optical microscopic view suggested the strong bond between dye and silk fabric that was influenced by time and temperature.

3.2.5 Thermogravimetric Analysis (TGA)

The thermal stability of the dyed and undyed silk fabric was determined using thermogravimetric analysis (TGA), as shown in Fig. 11a. The TGA analysis showed that the minimum amount of weight loss occurred between 72 and 230 °C for the dyed sample, and 62–262 °C for the undyed sample, respectively. In this region, the amount of amine group with different bonding groups stayed stable for both dyed and undyed silk fabric. During this stage of thermal degradation, the maximum weight loss occurred at 230–407 °C for dyed fabric and 262–382 °C for undyed silk fabric, respectively [47]. Thus, the major melting peak started at 230 and 262 °C, and it reached the melting point at 407 and 382 °C for dyed and undyed silk fabric, respectively. These TGA curves indicated that the melting peak point increased in the dyed sample. This TGA result was a symbol of strong molecular level interaction between Chinese fringe leaves dye and the fabric which was the result of bonding in the silk nanostructures [48]. Figure 11b exhibits the derivative thermogravimetric (DTG) curve for dyed and undyed silk fabrics where the maximum peak at the DTG curve was 325 and 320 °C, respectively, for the dyed and undyed samples. The higher DTG temperature indicated higher thermal stability. These DTG results clearly suggested that the undyed silk fabric showed less thermal stability as compared to dyed silk fabric. This derivative thermogravimetric (DTG) result was

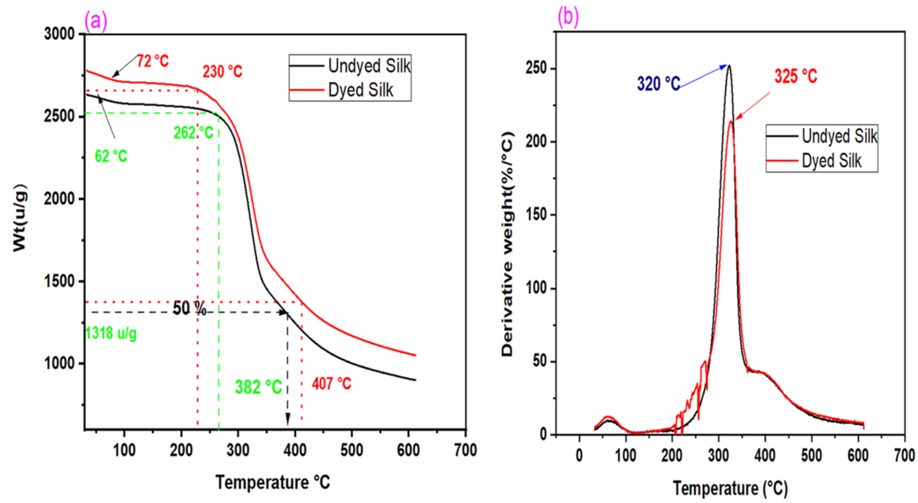

Fig. 11 **a** Thermogravimetric analyses (TGA) curves and **b** differential thermogravimetric (DTG) curves of dyed and undyed silk fabrics

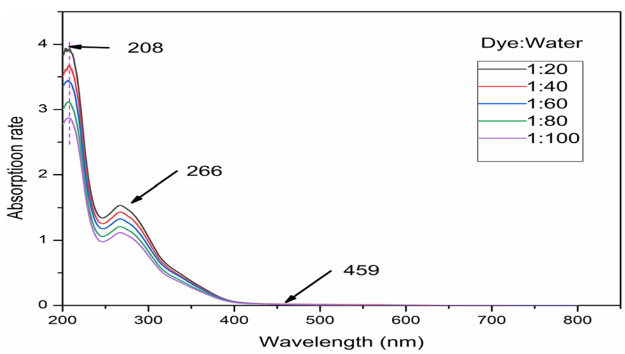

Fig. 12 UV–Vis spectra of Chinese fringe leaves extract dye solution (effect of extraction with a different material ratio)

in line with earlier researchers who verified the results' acceptance and accuracy [49].

3.2.6 Ultraviolet–Visible (UV–Vis) Spectroscopy Analysis of Dyes

Nowadays, UV–Vis spectroscopy is one of the most important tests for liquid samples. UV–Visible spectrum of Chinese fringe leaves extracted dye was evaluated with different material ratios and different pH where the range of wavelength was from 200 to 840 nm. Figure 12 displays the Ultraviolet–Visible spectroscopy of the dye solution where the wavelength of 200 to 208 nm for material ratios showed the highest absorption rate. The absorption rate went down to zero with the wavelength increased. The different material ratios were considered including 1:20, 1:40, 1:60, 1:80, and 1:100. According to Fig. 12, the material ratio of 1:20 showed maximum absorption rate value of 3.95 with a maximum wavelength of 208 nm. Hence, the best color absorption happened for the material ratio of 1:20. Another peak was observed at the wavelength of 266 cm^{-1}. Most of the ratios went to zero wavelength at 459 cm^{-1} [50]. The other factors such as temperature, pH, and time were not evaluated by this experiment. However, normally more temperatures occur in light to deep shade. In the case of dye extraction, the boiling temperature at 90 °C for 30 min was fixed for the full extraction process of Chinese fringe leaves dye. Thus, the best conditions for dye extraction was at M:L ratio of 1:20, temperature of 90 °C, pH of 4, and duration of 30 min. Additional temperature and more time caused dirty dye and filtering problem [51].

3.3 Proposed Dyeing Mechanism

A proposed reaction was introduced between silk fabric and dye of Chinese fringe leaves. He et al. revealed some chemical bonds and anthocyanin structures of Chinese fringe leaves in their previous study [52]. This proposed mechanism was created from FTIR analysis for both dye and silk fabric where the FTIR peak indicated there was present of functional groups in dye and silk fabric by forming ionic interactions with protonated amine groups ($R–NH_2$). In this dyeing process, the hydroxyl group and amino group were responsible for the absorption rate of dye by the combination of ionic bonds and hydrogen. Alkanin molecule and some functional groups created bonds with –OH, C–H, C–C, and NH_2 group [53]. The possible reaction between organic silk fabric and Chinese fringe leaves extracted dye has been shown in Scheme 3.

3.4 Properties of Silk-Treated Fabric

3.4.1 Air Permeability Analysis

The principle of air permeability is clearly illustrated in Scheme 4. This schematic diagram showed that some amounts of air were passed through fabric and some amounts

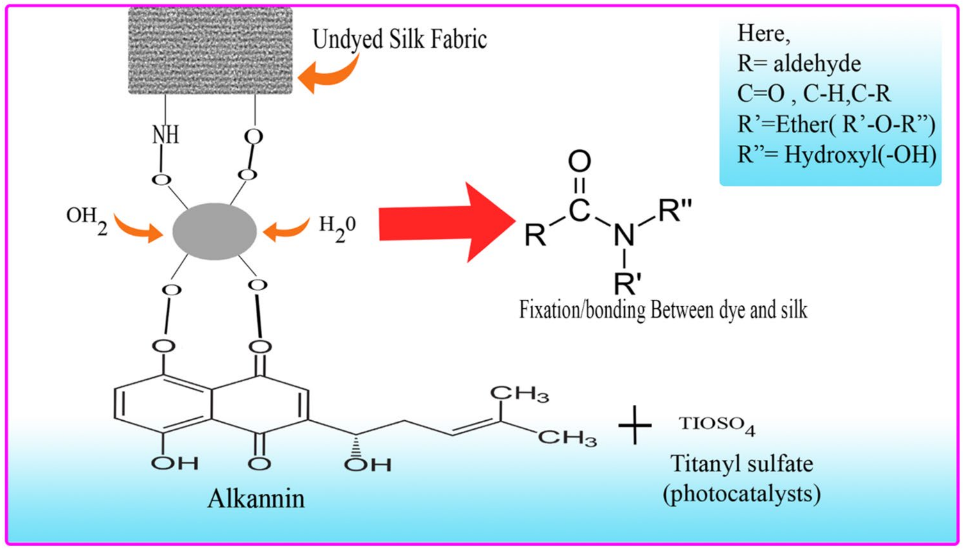

Scheme 3 Proposed mechanism for fixation between Chinese fringe tree leaves extracted dye and organic silk fabric

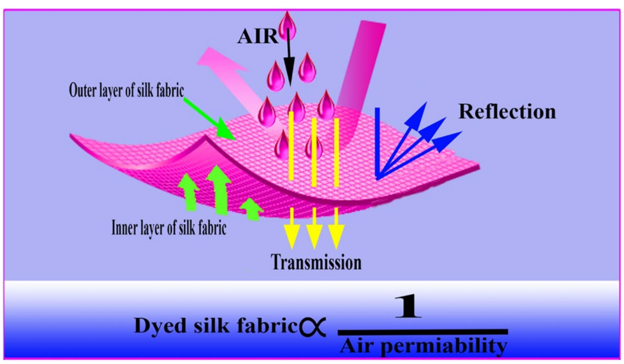

Scheme 4 Schematic diagram presented the working principle of air permeability

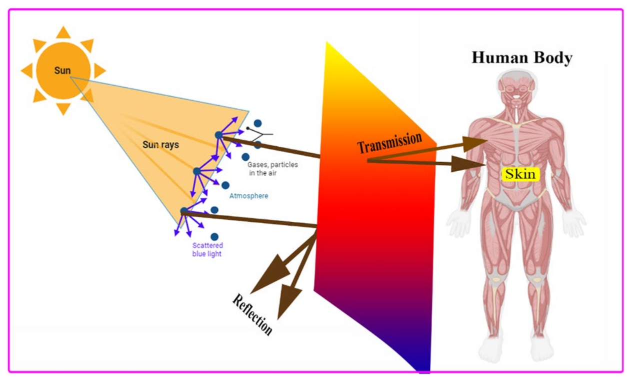

Scheme 5 A schematic diagram of UV and sun protection system principle

Table 6 Air permeability for dyed and undyed silk fabric

Sample type	Air permeability (mm/s)
Dyed silk fabric	122 ± 2
Undyed silk fabric	170 ± 2

of air were reflected form fabric layer. The air permeability value was decreased for dyed silk fabric. The air permeability values for the dyed and undyed silk fabric are listed in Table 6. The air permeability of undyed silk fabric was 170 ± 2 mm/s. On the other hand, the air permeability of the dyed sample was 122 ± 2 mm/s. The undyed silk fabrics exhibited somewhat a greater air permeability as compared to dyed silk fabric. This occurred because the dyeing process made the dyed silk fabric sample's pores less visible than undyed sample. Because the dyeing process of silk fabric nanostructure changed the silk fabric's pores. The value of air permeability changed according to dye intake of silk fabric. The more dye intake causes the more changes in molecular structure of silk fabric. That caused the less air passed through the dyed sample. According to the earlier research, this air permeability values reflected in an acceptable range [54].

3.4.2 Ultraviolet (UV) Protection Properties

Ultraviolet (UV) protection and sun ray are harmful for skin that can be dangerous for human skin [55]. Scheme 5 shows how the sun ray transmitted and reflected by the cloth layer to protect the harmful sun ray. Ultraviolet protection factor (UPF) value was used to measure the capacity to block the UV rays from the sun to protect human skin. Most of the textile dyes absorbed sunlight spectra in range of 400–700 nm [56]. Ultraviolet protection factor (UPF) values were evaluated with 4 grade where bad (<15), good (14–24), very good (25–39), and outstanding (> 40) [57]. Ultraviolet (UV) protection factor for dyed and undyed silk fabric is recorded in Table 7. Dyed fabric samples showed higher protection due to lower UVA and UVB transmittance [58]. Sun blocking properties raised due to the presence of dye in the fabric. The dyeing process changed their physical and chemical structure, and thus, raised the protection level [59]. The UPF value for the dyed samples was 95.50 that indicated excellent UV protection. On the other hand, UPF value of undyed silk fabric sample was 0.27, which indicated very poor UV protection. The structure of the dye molecule played an important role in UPF. The result of similar UV protection properties was observed by the other researchers [51].

3.4.3 Colorfastness Properties of Dyed Fabric

The ability to keep the color of textile materials intact in various adverse environments is called color fastness. The colorfastness properties of the dyed silk fabric samples are represented in Table 8. All the fabric samples performed very well to excellent (4–5 and 5) fastness properties. Overall, the dyed sample exhibited the maximum fastness properties due to the strong bonding between silk and dye molecules. Using a standard grey scale, the fastness properties (washing fastness, rubbing fastness, perspiration, and light fastness) were evaluated successfully [60, 61]. The washing fastness of the natural dye depended on the diffusion% (dye) and absorption of the dye. After washing the dyed silk fabric, it was observed with greyscale and found that there was a little color change and color staining in cotton for the silk fabric sample. Color staining for the samples showed maximum fastness properties. Similarly, after testing the rubbing fastness (dry and wet), it was found that the sample showed a little change in the greyscale. For perspiration fastness, there was a small change in the acidic medium. But for alkali medium, the dyed silk fabric presented very good to excellent fastness properties. For the light fastness properties, the dyed silk fabric samples exhibited the maximum fastness properties. All the fastness properties (different fabrics using different natural dyes) were verified by previous studies, as shown in Table 9 [62].

Table 7 UV protection properties of Chinese fringe leaves dyed silk fabric

Samples Type	UVA (%)	UVB (%)	Protection factor (UPF)	standard deviation (UPF Value)	Grading
Dyed silk fabric	0.34	0.31	317.9	95.50	Excellent
Undyed silk fabric	15.26	7.84	9.8	0.27	Very poor

Table 8 Color fastness to rubbing, perspiration, wash, and light of different dyed Silk fabric

Wash fastness							Rubbing		Perspiration		Light
Color change	Color Staining						Dry	Wet	Acidic	Alkaline	
	Acetate	Cotton	Nylon	Polyester	Acrylic	Wool					
4	5	4–5	5	5	5	5	4–5	4	4	4–5	5

Table 9 The comparison of different fabrics using different natural dyes

Fabric type	Natural dye	Wash fastness	Rubbing fastness		Perspiration fastness		Light Fastness	References
		Color change	Dry	Wet	Acidic	Alkaline		
Silk	Chinese fringe leaves	4	4–5	4	4	4–5	5	This work
Cotton fabric	Mango peel	4	4–5	4–5	–	–	5	[43]
Silk	Pterocarpus indicus Willd	4	4	4	4	4	4	[63]
Silk	Ipomoea batatas leaves	5	5	4–5	–	–	5	[64]
Polyester fabric	Ipomoea batatas leaves	5	5	4–5	–	–	4	[64]
Polyester fabric	Henna leaves	5	5	4	5	4–5	–	[45]
Cotton fabric	Turmeric powder	4	4	3–4	4	3–4	–	[65]

Table 10 Cost of silk fabric dyeing with Chinese fringe leaves extracts (US dollars) for processing per kg of silk fabric

No	Type of costing	Cost (USD $) per kg of silk fabric
1	Collection of waste leaves and cleaning them properly to be ready for grinding	0.26
2	Titanyl sulfate (2% (o.w.f.))	0.11
3	Dyeing procedure	0.56
	Total	0.93

4 Cost Analysis of Silk Fabric Dyeing with Chinese Fringe Leaf Extract

The approximate cost analysis for the silk fabric dyeing process with Chinese fringe leaves is presented in Table 10. The total dyeing process was significantly at the lowest price compared to other dyeing process. Shahid et al. revealed the cost analysis of wool yarn with pomegranate peel extract in a recent study [66]. However, the cost of that eco-friendly natural dyeing was higher than the synthetic dyeing process. To confirm the ecological and environmental benefits of their low toxicity, aesthetic qualities, and their relatively high-cost performance in comparison to synthetic dyes might be compromised. In addition, the resource that ultimately led to the economical use of waste materials, as a renewable raw material for textile material coloring ensured a "sustainable cleaner production" approach for waste disposal. Since most of the Chinese fringe leaves were cut off and discarded as waste each month.

5 Conclusions

The key focus of this study was to explore sustainable and environmentally friendly methods for dyeing silk fabric using extracts from Chinese fringe leaves. Various scientific experiments, including SEM, FTIR, optical microscopy, air permeability, UV, and sun protection tests were conducted to achieve the research goals. The conventional extraction method yielded the best results in terms of color strength and colorimetric properties, attributed to the abundance of coloring groups such as auxochrome and chromophore in Chinese fringe leaves. Manipulating dye dosage, temperature, and dyeing time allowed for variations in shade depth, with higher doses and temperatures resulting in darker shades. Taguchi analysis identified optimal dyeing conditions, with initial and predicted *K/S* values indicating successful dye uptake. Dyeing at 90 °C for 90 min with a 20% dye dosage demonstrated superior color strength. Besides, increased dyeing parameters led to molecular changes in the fabric, suggesting enhanced nanoparticle interactions without the need for mordants. FTIR analysis revealed distinct bonds in the silk fabric, indicating successful dye absorption. Morphological evaluations showed minor surface alterations in dyed fabric samples compared to undyed ones, without any signs of damage. Dyed silk fabric exhibited less air permeability, and excellent UV and sun protection properties with a UPF of 95.50, highlighting its potential for practical use. Moreover, the utilization of waste materials for dye extraction contributed to sustainability by minimizing chemical usage and wastewater generation. In conclusion, Chinese fringe leaves offered significant potential for sustainable coloration of silk fabrics without resorting to harmful chemicals. This research underscored the feasibility of eco-friendly dyeing processes in the textile industry.

Supplementary Information The online version contains supplementary material available at https://doi.org/10.1007/s12221-024-00836-6.

Acknowledgements We extend our heartfelt gratitude to Professor Haroon A. M. Saeed at Wuhan Textile University, China for managing all the funding for this study. We would also like to thank Assistant Professor Dr. Syed Rashedul Islam from Uttara University, Bangladesh, and Aimal Khan from Wuhan Textile University, China for their invaluable guidance in successfully completing this research.

Author contributions Md Shazzat Hossain: data analysis testing, writing—review and editing; Syed Rashedul Islam: supervising, writing—review and editing resources, and revising the manuscript; Yahui Zhou: methodology, testing, writing—review and editing resources; Haroon A.M. Saeed: funding, review and supervising; Aimal khan: review and correction.

Data availability statement All data included in the study are available upon request by contact with the corresponding author.

Declarations

Conflict of interest The authors state that none of the work presented in this study may have been influenced by any known conflicting financial interests or personalities.

References

1. G.E. Motta, M. Angonese, G. Ayala Valencia, S.R.S. Ferreira, Sustain. Chem. Pharm. **30**, 100893 (2022)
2. R. Kumar, A. Verma, A. Shome, R. Sinha, S. Sinha, P.K. Jha, R. Kumar, P. Kumar, Shubham, S. Das, P. Sharma, P.V. Vara Prasad, Sustainability **13**, 9963 (2021)
3. A. Raj, A. Chowdhury, S.W. Ali, Sustain. Chem. Pharm. **27**, 100689 (2022)
4. T. Islam, Md.R. Repon, T. Islam, Z. Sarwar, M.M. Rahman, Environ. Sci. Pollut. Res. **30**, 9207 (2022)
5. F.R. Abe, J.N. Mendonça, L.A.B. Moraes, G.A.R.D. Oliveira, C. Gravato, A.M.V.M. Soares, D.P.D. Oliveira, Chemosphere **178**, 282 (2017)
6. J. Sharma, S. Sharma, V. Soni, Reg. Stud. Mar. Sci. **45**, 101802 (2021)
7. G. Mastrangelo, U. Fedeli, E. Fadda, G. Milan, J.H. Lange, Toxicol. Ind. Health **18**, 171 (2002)
8. M. Younis, S. Adeel, M.Z. Haider, R. Mia, M. Imran, Sustain. Chem. Pharm. **37**, 101410 (2024)

9. J.M. Jabar, K.M. Al-Ahmary, I.F. Alshdoukhi, A.A. Alghamdi, A. El-Rayyes, M.R. Alrahili, Sustain. Chem. Pharm. **39**, 101587 (2024)
10. A. Rehman, A. Ahmad, A. Hameed, S. Kiran, T. Farooq, Sustain. Chem. Pharm. **21**, 100432 (2021)
11. A. Kushwaha, S. Singh, K. Chaudhary, Sustain. Chem. Pharm. **34**, 101146 (2023)
12. F.-S. Li, J.-K. Weng, Nat. Plants **3**, 17109 (2017)
13. S.M. Ghoreishian, L. Maleknia, H. Mirzapour, M. Norouzi, Fibers Polym. **14**, 201 (2013)
14. Y. Ding, H.S. Freeman, Color. Technol. **133**, 369 (2017)
15. F.U. Rehman, S. Adeel, W. Haddar, R. Bibi, M. Azeem, R. Mia, B. Ahmed, Sustainability **14**, 5599 (2022)
16. W. Zhang, X. Wang, Y. Zhang, S. Wu, R. Liu, Sustain. Chem. Pharm. **28**, 100708 (2022)
17. X. Zhang, L. Zhang, D. Zhang, D. Su, W. Li, X. Wang, Q. Chen, W. Cai, L. Xu, F. Cao, D. Zhang, X. Yu, Y. Li, BMC Plant Biol. **23**, 133 (2023)
18. A. Khan, M.T. Hussain, H. Jiang, Color. Technol. **134**, 266 (2018)
19. A. Khan, M.T. Hussain, H. Jiang, S. Gul, J. Nat. Fibers **17**, 472 (2020)
20. M.G. Uddin, J. Text. **2014**, 405626 (2014). https://doi.org/10.1155/2014/405626
21. M.G. Uddin, Text. Cloth. Sustain. **1**, 7 (2015)
22. K.L. Do, M. Su, A. Mushtaq, F. Zhao, Fibers Polym. **24**, 2773 (2023)
23. N. Punrattanasin, M. Nakpathom, B. Somboon, N. Narumol, N. Rungruangkitkrai, R. Mongkholrattanasit, Ind. Crops Prod. **49**, 122 (2013)
24. T.B. Teklemedhin, L.H. Gopalakrishnan, J. Text. Sci. Eng. **S3**, 001 (2018). https://doi.org/10.4172/2165-8064.S3-001
25. H. Dayioglu, D. Kut, N. Merdan, S. Canbolat, Proc. Soc. Behav. Sci. **195**, 1609 (2015)
26. P. Sasivatchutikool, M. Nakpathom, Fibers Polym. **20**, 1841 (2019)
27. W. Rasool, S. Adeel, F. Batool, S.A. Ahmad, S. Mumtaz, M. Hussaan, Environ. Sci. Pollut. Res. **30**, 21863 (2022)
28. K. Iqbal, H. Afzal, M.O.R. Siddiqui, U. Bashir, K. Jan, A. Abbas, H.A. Abid, Sustain. Chem. Pharm. **33**, 101094 (2023)
29. M.R. Sohrabi, A. Khavaran, S. Shariati, S. Shariati, Arab. J. Chem. **10**, S3523 (2017)
30. Md.N. Pervez, W.S. Yeo, L. Lin, X. Xiong, V. Naddeo, Y. Cai, Sci. Rep. **13**, 12363 (2023)
31. D. Fratila, C. Caizar, J. Cleaner Prod. **19**, 640 (2011)
32. R. Alcaraz de la Osa, I. Iparragirre, D. Ortiz, J.M. Saiz, ChemTexts **6**, 2 (2019)
33. M.A.R. Bhuiyan, M.M. Rahman, A. Shaid, M.M. Bashar, M.A. Khan, J. Cleaner Prod. **112**, 3063 (2016)
34. L. Lin, T. Jiang, L. Li, Md.N. Pervez, C. Zhang, C. Yan, Y. Cai, V. Naddeo, Sci. Rep. **12**, 13833 (2022)
35. Md.Y. Hossain, Y. Liang, Md.N. Pervez, X. Ye, X. Dong, M.M. Hassan, Y. Cai, Cellulose **28**, 517 (2021)
36. I. Hossain, A. Hossain, I.A. Choudhury, J. Text. Inst. **107**, 154 (2016)
37. Md. Pervez, F. Shafiq, Z. Sarwar, M. Jilani, Y. Cai, Materials **11**, 426 (2018)
38. D. Sudhakara, G. Prasanthi, J. Inst. Eng. India Ser. C **98**, 119 (2017)
39. T. Hussain, S. Ali, F. Qaiser, Color. Technol. **126**, 256 (2010)
40. V. Rotich, P. Wangila, J. Cherutoi, J. Chem. **2022**, 2233414 (2022). https://doi.org/10.1155/2022/2233414
41. M. Mecozzi, M. Pietroletti, M. Scarpiniti, R. Acquistucci, M.E. Conti, Environ. Monit. Assess. **184**, 6025 (2012)
42. M. Puchalska, M. Orlińska, M.A. Ackacha, K. Połeć-Pawlak, M. Jarosz, J. Mass Spectrom. **38**, 1252 (2003)
43. M. Ayele, T. Tesfaye, D. Alemu, M. Limeneh, B. Sithole, Chem. Pharm. **17**, 100293 (2020)
44. A.A. Abd El Aty, G.T. El-Bassyouni, N.A. Abdel-Zaher, O.W. Guirguis, Fibers Polym. **19**, 1880 (2018)
45. M.A. Rahman Bhuiyan, A. Ali, A. Islam, M.A. Hannan, S.M. Fijul Kabir, M.N. Islam, Fash. Text. **5**, 2 (2018)
46. N.A. Ibrahim, W.A. El-Sayed, N.A. Ameen, Color. Technol. **126**, 289 (2010)
47. N.A. El-Zaher, G.T. El-Bassyouni, M.A. Esawy, O.W. Guirguis, J. Nat. Fibers **18**, 1247 (2021)
48. S.R. Islam, A. Alassod, M.K. Patoary, T. Naveed, M.A. Ali, J. Jiang, AATCC J. Res. **8**(5), 11 (2021). https://doi.org/10.14504/ajr.8.5.2
49. C. Dorina, M. Dochia, S. Gavrilas, Rev. Roum. Chim. **64**, 453 (2019). https://doi.org/10.33224/rrch/2019.64.5.09
50. G. Shanker, G. Hegde, C. Rodriguez-Abreu, Liq. Cryst. **43**, 473 (2016)
51. R. Mia, Md. Minhajul Islam, T. Ahmed, Md. Azhar Waqar, N. Jahan Khanam, S. Sultana, Md. Sajjadul Karim Bhuiyan, Md. Nizam Uddin, Clean. Eng. Technol. **8**, 100471 (2022)
52. C. He, Y. Jiang, H. Fang, Y. Zhang, Z. Guo, ChemRxiv, 2020. https://doi.org/10.26434/chemrxiv.13148705.v1
53. S. Fazal-ur-Rehman, S. Adeel, M. Liaqat, R. Hussaan, B. Mia, H. Ahmed, Ind. Crops Prod. **186**, 115301 (2022)
54. R.T. Ogulata, S. (Mavruz) Mezarcioz, J. Text. Inst. **103**, 654 (2012)
55. J. Aguilera, E. Navarrete-de Gálvez, C. Sánchez-Roldán, E. Herrera-Ceballos, M.V. De Gálvez, Photochem. Photobiol. **99**, 184 (2023)
56. O.K. Alebeid, T. Zhao, J. Text. Inst. **108**, 2027 (2017)
57. N. Nasirzadeh, M. Monazam Esmaeelpour, N. Naseri, S. Omari Shekaftik, Int. J. Environ. Health Res. **34**, 2067 (2023)
58. K. Gong, Y. Pan, L.J. Rather, W. Wang, Q. Zhou, T. Zhang, Q. Li, Dyes Pigm. **166**, 114 (2019)
59. S.A. Noorian, N. Hemmatinejad, A. Bashari, Photochem. Photobiol. **91**, 510 (2015)
60. M.A.R. Bhuiyan, A. Islam, A. Ali, M.N. Islam, J. Cleaner Prod. **167**, 14 (2017)
61. J.M. Jabar, I.A. Owokotomo, A.F. Ogunsade, Sustain. Chem. Pharm. **29**, 100822 (2022)
62. Y.-H. Lee, H.-D. Kim, Fibers Polym. **5**, 303 (2004)
63. N. Kandasamy, K. Kaliappan, T. Palanisamy, Ind. Crops Prod. **171**, 113969 (2021)
64. J. Fang, C. Meng, G. Zhang, Ind. Crops Prod. **177**, 114440 (2022)
65. Md.D. Hosen, Md.F. Rabbi, Md.A. Raihan, Md.A. Al Mamun, Clean. Eng. Technol. **3**, 100124 (2021)
66. M. Shahid, Shahid-ul-Islam, L.J. Rather, N. Manzoor, F. Mohammad, J. Nat. Fibers **16**, 555 (2019)